



Cite this: *Green Chem.*, 2022, **24**, 9027

Received 11th August 2022,
Accepted 28th October 2022

DOI: 10.1039/d2gc02990a

rsc.li/greenchem

Redox-neutral synthesis of π -allylcobalt complexes from alkenes for aldehyde allylation via photoredox catalysis†

Dandan Zhang,^a Haoyu Li,^a Zhuowen Guo,^a Yuqing Chen,^a Huaipu Yan,^a Zenghui Ye,^b Fengzhi Zhang,^{id} *^b Binghui Lu,^c Erjun Hao^{id} ^c and Lei Shi^{id} *^{a,c}

This work reports the first visible-light mediated cobalt-catalyzed aldehyde allylation with simple alkenes to produce homo-allylic alcohols. This novel strategy directly uses easily available unactivated alkenes as alternative allyl sources instead of pre-synthesized allylic halides/alcohols, thus bypassing the need for exogenous reductants. Mechanistic studies suggest that the unprecedented combination of allyl radical intermediates and Co^I species to generate nucleophilic π -allylcobalt^{II} under photoredox conditions represents the key step in the catalytic cycle.

Introduction

The development of sustainable synthetic strategies for the direct conversion of feedstock chemicals into high value-added fine products with atom economy is at the core of current organic chemistry.^{1,2} The addition of various π -allylmethyl species to carbonyls remains the most powerful and reliable method for the synthesis of homo-allylic alcohols.^{3–7} However, pre-synthesized allylic halides/esters are used, and excessive amounts of stoichiometric reductants are necessary to regenerate nucleophilic π -allylmethyl species, suggesting the need for sustainable improvement. Against this backdrop, the direct allylic C(sp³)-H functionalization of abundant and easily available alkenes has attracted considerable attention due to its overall synthetic efficiency.^{8,9}

Among various transition metals, cobalt is an Earth-abundant and inexpensive transition metal with low toxicity.^{10,11} In addition, its rich redox potential facilitates sustainable organic synthesis.^{12,13} Since the early 20th century, cobalt has played a

major role in fundamental industrial processes such as hydroformylation and the Fischer-Tropsch process.^{14,15} Its key applications in modern organic chemistry are multiple, including the Pauson-Khand reaction,¹⁶ hydrogenation,¹⁷ C-H activation,¹⁸ and so on. However, cobalt is rarely used in carbonyl allylation.¹⁹ Mita, Sato, and co-workers reported a cobalt/Xantphos system with AlMe₃ for the allylation of ketones with terminal alkenes.^{20,21} Most recently, the first photoredox and Co-catalyzed reductive carbonyl allylation was reported independently by Cozzi, Kleij, and our group.^{22,23,24–26} In particular, Kleij *et al.* developed the elegant synthesis of *syn*-1,3-diols via Co/organophotoredox dual catalysis with extensive mechanism studies (Scheme 1a).^{24–26} Additionally, Xia *et al.* disclosed a photoredox/Co-catalyzed highly regio- and enantioselective reductive coupling of alkynes and aldehydes.²⁷ Xiao *et al.* reported an elegant photocatalytic Co-catalyzed asymmetric reductive Grignard-type addition of aryl iodides to aldehydes.^{28,29} Furthermore, Meng *et al.* reported an enantioselective Co-catalyzed aldehyde allylation with an exceptional substrate scope.^{30,31–36} To date, presynthesized allylic halides/esters and excessive reductants are required for Co-catalyzed carbonyl allylation.

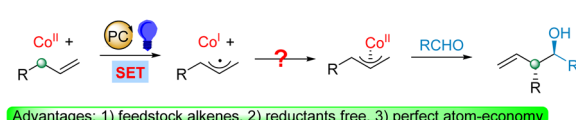
In recent years, metallaphotoredox catalysis has been used to perform various unconventional organic transformations by

a) Classical synthesis of nucleophilic π -allylmethyl complexes for allylation



Limitations: 1) pre-synthesized allyl acetate, 2) excess wastes, 3) poor atom-economy

b) This work: redox-neutral generation of nucleophilic π -allyl-Co(II) from alkenes



Advantages: 1) feedstock alkenes, 2) reductants free, 3) perfect atom-economy

Scheme 1 Strategies for the synthesis of nucleophilic π -allylmethyl species for carbonyl allylation.

^aZhang Dayu School of Chemistry, Dalian University of Technology, Dalian, Liaoning, 116024, China. E-mail: shilei17@dlut.edu.cn

^bSchool of Pharmaceutical Sciences, Hangzhou Medical College, Hangzhou, Zhejiang, 310059, China. E-mail: fengzhi_zhang@hotmail.com

^cSchool of Chemistry and Chemical Engineering, Henan Normal University, Xinxiang, Henan, 453007, China

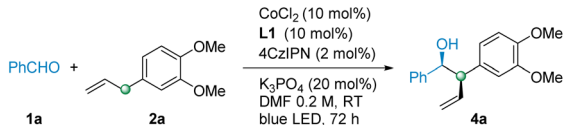
† Electronic supplementary information (ESI) available. See DOI: <https://doi.org/10.1039/d2gc02990a>

activating inert substrates.^{37–41} To further improve the sustainability, and inspired by the recent outstanding studies of Glorius and Kanai on photoredox and Cr catalysis,^{42–44} we investigated whether metallaphotoredox dual catalysis could be an alternative and sustainable strategy to access π -allylcobalt complexes from feedstock alkenes in a redox-neutral manner (Scheme 1b).^{13,45–49} We envisaged that photocatalyst-mediated single electron transfer (SET) between alkene and Co^{II} could generate a radical pair of allyl radical and Co^I, which would further recombine into π -allylcobalt complexes for carbonyl allylation. Herein, we report the first successful redox-neutral synthesis of π -allylcobalt complexes from alkenes for aldehyde allylation, obviating the need for stoichiometric reductants or activation reagents and thus contributing to perfect atom-economy and environmental sustainability.

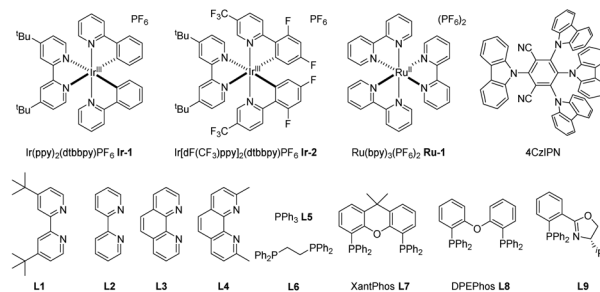
Results and discussion

Reaction optimization studies were initiated using benzaldehyde **1a** and electron-rich 1,2-dimethoxy-4-allylbenzene **2a** as standard substrates (Table 1). Extensive screening revealed that the optimised reaction conditions were: CoCl₂ (10 mol%) combined with 4,4'-di-*tert*-butylbipyridine (**L1**, 10 mol%), 2,4,5,6-tetra(9*H*-carbazol-9-yl)isophthalonitrile (**4CzIPN**, 2 mol%), and K₃PO₄ (20 mol%) in DMF under irradiation with a blue LED at room temperature for 72 hours. The homoallylic alcohol **4a** was obtained in a satisfactory yield of 91% with decent regio- and diastereoselectivity (dr = 8 : 1, Table 1, entry 1). Notably, the reaction parameters significantly affected the reaction outcome. As shown in Table 1, while various Co salts failed to catalyze the reaction, CoBr₂ facilitated the process, although the diastereoselectivity was low (dr = 5 : 1, entries 2 and 3). Ligands were found to be important for allylation. When bipyridine **L2** was used, the yield slightly decreased to 89% with similar diastereoselectivity (dr = 8 : 1, entry 4). However, phosphor ligands did not promote the reaction (entry 5). Reactions were also highly sensitive to solvents. Using various solvents such as CH₃CN, CH₂Cl₂, THF, DMSO, DMF, and DCE resulted in reduced yields and poor diastereoselectivities (entries 6–10). Further screening of other photocatalysts revealed that Ir(ppy)₂(dtbbpy)PF₆ (**Ir-1**) and Ir[dF(CF₃)ppy]₂(dtbbpy)PF₆ (**Ir-2**) catalyzed the reaction but afforded **4a** in lower yields (entries 11–13). Furthermore, the reaction did not proceed in the absence of a ligand, a photocatalyst, or light (entries 14–16). We noticed that in the absence of the catalyst Co, **4a** was obtained in 15% yield but with no diastereoselectivity, indicating that a background reaction occurred (entry 17). Interestingly, in the absence of base additives, allylic alcohol **4a** was obtained in a yield of 66%, but with only a 4 : 1 dr (entry 18). This result indicated that base additives have a significant impact on diastereoselectivity. Additionally, condition-based sensitivity testing showed that the reaction was sensitive to H₂O and a high oxygen concentration.

Table 1 Reaction optimization^{a,b,c}

		
Entry	Variation from standard conditions	Yield (%)
1	None	91 (dr = 8 : 1)
2	CoBr ₂	76 (dr = 5 : 1)
3	CoSO ₄ , Co(acac) ₂ , Co(OAc) ₂ , Co(NO ₃) ₂	0
4	L2	89 (dr = 8 : 1)
5	L3–L9	0
6	CH ₃ CN	16 (dr = 5 : 1)
7	CH ₂ Cl ₂	7 (dr = 1.6 : 1)
8	THF	Trace
9	DMSO	20 (dr = 1.2 : 1)
10	DCE	12 (dr = 4 : 1)
11	Ir-1 instead of 4CzIPN	48 (dr = 4 : 1)
12	Ir-2 instead of 4CzIPN	74 (dr = 6 : 1)
13	Ru-1 instead of 4CzIPN	Trace
14	No ligand L1	Trace
15	No 4CzIPN	0
16	No light	0
17	No Co	15 (dr = 1 : 1)
18	No K ₃ PO ₄	60 (dr = 4 : 1)

^a Reaction conditions: **1a** (0.5 mmol scale). ^b Yields were determined by ¹H NMR spectroscopy versus dimethyl terephthalate as an internal standard. ^c Diastereomeric ratios were determined by ¹H NMR spectroscopy of crude products.



After establishing the optimal reaction conditions, we analyzed the scope of the allylation reactions (Table 2). The redox-neutral Co-catalysis system was generally active during allylation with diverse aromatic and aliphatic aldehydes, affording homoallylic alcohols in good to excellent yields with acceptable regio- and diastereoselectivity. Both primary and secondary aldehydes facilitated allylation with generally satisfactory yields and diastereoselectivities (**3a–3f**). However, tertiary pivalaldehyde failed to react, probably due to the large steric hindrance. Notably, the terminal chlorine atom on the alkyl chain (**3c**) was successfully preserved under mild redox-neutral conditions. The catalytic system was sensitive to the electrical properties of the substituents on the aromatic ring. Both electron-rich groups, such as methoxyl **4m** and methylthio **4j**, and electron-withdrawing groups, such as fluorine **4d** and trifluoromethyl **4f**, yield homoallylic alcohols with comparable diastereoselectivities. The sterically hindered mesitylaldehyde **4i** was subjected to allylation. Heteroatoms such as the pro-

Table 2 Scope of allylation reactions^{a,b}

<div><div><div>RCHO</div><div>1</div></div><div>+</div><div><div><div><div>Ar/NPh₂</div><div>2</div></div><div><div>Co</div><div>PC</div></div><div><div>K₃PO₄</div><div>DMF</div><div>RT</div></div></div><div><div><div>R</div><div>OH</div><div>Ar/NPh₂</div><div>3,4,5,6</div></div></div></div></div>					
Scope of Aliphatic Aldehydes					
<div><div><div><div><div></div><div>3a</div></div><div>70% d.r.=10:1</div></div></div></div>	<div><div><div><div><div>F₃C</div><div>3b</div></div><div>70% d.r.=9:1</div></div></div></div>	<div><div><div><div><div>Cl</div><div>3c</div></div><div>50% d.r.=13:1</div></div></div></div>	<div><div><div><div><div></div><div>3d</div></div><div>67% d.r.=15:1</div></div></div></div>	<div><div><div><div><div></div><div>3e</div></div><div>64% d.r.=10:1</div></div></div></div>	<div><div><div><div><div>BocN</div><div>3f</div></div><div>67% d.r.=7:1</div></div></div></div>
Scope of Aryl Aldehydes					
<div><div><div><div><div></div><div>4a</div></div><div>88% d.r.=8:1</div></div></div></div>	<div><div><div><div><div>Ph</div><div>4b</div></div><div>92% d.r.=8:1</div></div><div>1.56 g, 87% yield</div><div>d.r.=8:1</div></div></div>	<div><div><div><div><div></div><div>4c</div></div><div>90% d.r.=10:1</div></div></div></div>	<div><div><div><div><div>F</div><div>4d</div></div><div>50% d.r.=7:1</div></div></div></div>	<div><div><div><div><div>Cl</div><div>4e</div></div><div>91% d.r.=5.6:1</div></div></div></div>	<div><div><div><div><div>F₃C</div><div>4f</div></div><div>55% d.r.=4:1</div></div></div></div>
<div><div><div><div><div>Me</div><div>4g</div></div><div>75% d.r.=10:1</div></div></div></div>	<div><div><div><div><div>Me</div><div>4h</div></div><div>87% d.r.=8:1</div></div></div></div>	<div><div><div><div><div>Me</div><div>4i</div></div><div>54% d.r.=13:1</div></div></div></div>	<div><div><div><div><div>MeS</div><div>4j</div></div><div>64% d.r.=9.3:1</div></div></div></div>	<div><div><div><div><div>MeO</div><div>4k</div></div><div>78% d.r.=9.7:1</div></div></div></div>	<div><div><div><div><div>MeO</div><div>4l</div></div><div>53% d.r.=8:1</div></div></div></div>
<div><div><div><div><div>MeO</div><div>4m</div></div><div>56% d.r.=5:1</div></div></div></div>	<div><div><div><div><div></div><div>4n</div></div><div>90% d.r.=7:1</div></div></div></div>	<div><div><div><div><div></div><div>4o</div></div><div>93% d.r.=10:1</div></div></div></div>	<div><div><div><div><div></div><div>4p</div></div><div>80% d.r.=4:1</div></div></div></div>	<div><div><div><div><div>Me</div><div>4q</div></div><div>79% d.r.=10:1</div></div></div></div>	<div><div><div><div><div></div><div>4r</div></div><div>51% d.r.=5:1</div></div></div></div>
<div><div><div><div><div>Ac</div><div>4s</div></div><div>73% d.r.=12:1</div></div></div></div>	<div><div><div><div><div></div><div>4t</div></div><div>82% d.r.=4:1</div></div></div></div>	<div><div><div><div><div>conjugated aldehyde</div></div></div></div></div>	<div><div><div><div><div></div><div>4u</div></div><div>55% d.r.=4:1</div></div></div></div>	<div><div><div><div><div></div><div>4v</div></div><div>75% d.r.=13:1</div></div></div></div>	<div><div><div><div><div>Ar₁ = <div><div><div><div>OMe</div><div>OMe</div></div></div></div></div></div></div></div></div>
<div><div><div><div><div></div><div>5a</div></div><div>93% d.r.=14:1</div></div></div></div>	<div><div><div><div><div></div><div>5b</div></div><div>74% d.r.=6:1</div></div></div></div>	<div><div><div><div><div></div><div>5c</div></div><div>94% d.r.=7:1</div></div></div></div>	<div><div><div><div><div></div><div>5d</div></div><div>62% d.r.=7:1</div></div></div></div>	<div><div><div><div><div></div><div>5e</div></div><div>51% d.r.=7:1</div></div></div></div>	
<div><div><div><div><div>F</div><div>5f</div></div><div>65% d.r.=3:1</div></div></div></div>	<div><div><div><div><div></div><div>5g</div></div><div>63% d.r.=5:1</div></div></div></div>	<div><div><div><div><div></div><div>5h</div></div><div>87% d.r.=14:1</div></div></div></div>	<div><div><div><div><div></div><div>5i</div></div><div>86% d.r.=10:1</div></div></div></div>	<div><div><div><div><div></div><div>5j</div></div><div>40% d.r.=5:1</div></div></div></div>	
late-stage functionalization of structurally complex molecules					
<div><div><div><div><div>from bezafibrate</div><div>6a</div></div><div>75% d.r.=8:1</div></div></div></div>	<div><div><div><div><div>from febuxostat</div><div>6b</div></div><div>70% d.r.=8:1</div></div></div></div>	<div><div><div><div><div>from oxaprozin</div><div>6c</div></div><div>88% d.r.=8:1</div></div></div></div>			

^a Isolated yields of two diastereoisomers. Reactions were performed at the 0.5 mmol scale for **1** (1 eq. DMF 0.2 M), **2** (3 eq.), 4CzIPN (2 mol%), CoCl₂ (10 mol%), **L1** (10 mol%), and K₃PO₄ (20 mol%) in the presence of a blue LED for 72 hours (for details see ESI S3†). ^b Diastereomeric ratios were determined by ¹H NMR spectroscopy of crude products.

tested amine **3f** did not interfere with the catalytic cycle. Heteroarenes are frequently found in the core structures of natural products and pharmaceuticals. The newly developed

method showed impressive compatibility with various heteroarenes, such as furans **4n**, **4o**, and **4q**, thiophenes **4p** and **4r**, and 5-methoxyindole **4s**. However, the presence of the pyridine

group **4t** resulted in a low diastereoselectivity (4 : 1) but a high yield (82%), indicating that the nitrogen atoms on pyridine exhibit strong coordination properties and possibly interact with metallic cobalt. Furthermore, the synthesis from highly active conjugated aldehydes, which were challenging substrates in the previous strategy, was facilitated to successfully afford **4u** and **4v**. The substrates can be extended to additional alkoxyated allyl-benzenes such as **5a–5d**, where the benzyloxy group could be deprotected under mild conditions to generate

a free hydroxy group. Nitrogen-containing substrates such as *N*-allyl-diarylamine were successfully used to obtain the desired 1,2-amino alcohols (**5e–5g**). To determine the scalability of the reaction, a gram-scale synthesis of **4b** was performed under the standard conditions. Satisfactorily, product **4b** was obtained in 87% yield (1.56 g) without deterioration. The mild photocatalytic and redox-neutral conditions provide a great opportunity for potential application in the late-stage functionalization of structurally complex molecules, including bezafibrate, febuxostat, and oxaprozin derivatives. The desired products **6a–6c** were obtained in decent yields. The use of the Earth-abundant cobalt, broad compatibility with sensitive functional groups, and simple reaction conditions are conducive to laboratory and industrial applications.

A series of mechanistic experiments were performed to investigate the active intermediates in the catalytic cycle. First, radical trapping studies indicated that the reactions were greatly inhibited by the addition of TEMPO (2,2,6,6-tetramethylpiperidinyloxy) as a radical scavenger (Fig. 1). The radical-capturing reaction resulting in the formation of adducts **10a-1** (or **10a-2**) was confirmed by mass spectrometry *via* careful analyses of crude reaction mixtures. Thus, the allyl radical **10a** was indeed generated *via* the radical cation [**2a**]^{•+}

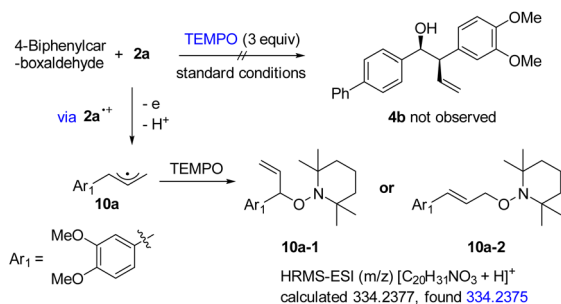


Fig. 1 TEMPO trapping experiments (for details please see ESI S8†).

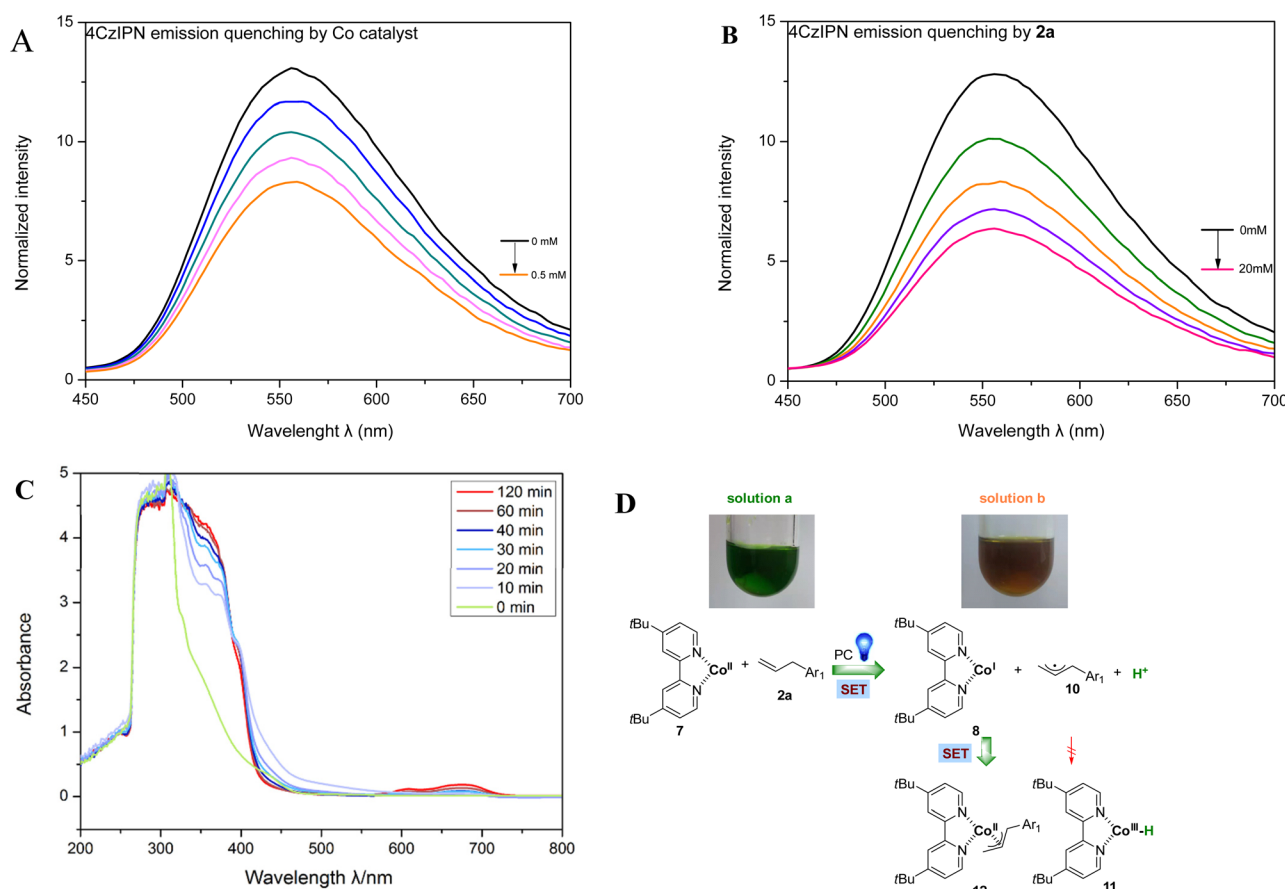


Fig. 2 (A and B) 4CzIPN emission quenching by the Co catalyst and **2a**. (C) UV-vis spectroscopy of cobalt species in the reaction. (D) Possible Co species in the reaction (for details please see ESI S7†).

by the sequential loss of an electron and a proton under photo-irradiation, suggestive of the radical nature of the reaction.

Stern–Volmer luminescence quenching studies were conducted to probe the SET between the photocatalyst and the reaction substrates (Fig. 2A and B). These studies showed that both LnCo^{II} **7** and allylbenzene **2a** can readily quench the luminescence of 4CzIPN. The higher concentration of **2a** compared to that of the Co catalyst in the reaction suggests the strong feasibility of reductive quenching of the excited state of 4CzIPN with **2a**.

UV-vis spectroscopy studies were also carried out to obtain further insight into the reaction mechanism (ESI S7†). CoBr_2 , **L1**, K_3PO_4 , and 4CzIPN were added into a solution of DMF (Fig. 2D, solution a). Initially, no color changes of the resulting mixture were observed in the dark even at higher temperatures, indicating that the ground-state SET cannot take place. However, when the mixture was irradiated with a 450 nm LED, the color changed gradually from green to brown within 120 minutes (Fig. 2D, solution a to b). Simultaneously, the UV-vis spectroscopic analysis of the reaction revealed that a strong absorption band at 350–460 nm appeared rapidly in about 20 minutes, and another weak but broad absorption band at 580–720 nm appeared eventually (Fig. 2C). All these data clearly suggest the occurrence of a photo-induced electron transfer with the generation of new Co species. The broad absorption band at 580–720 nm might be suggestive of the presence of a small number of LnCo^{I} **8** species, which is consistent with previous studies.^{23,30,50,51} LnCo^{I} **8** may undergo oxidation by protons to generate $\text{LnCo}^{\text{III}}\text{-H}$ **11**,^{13,46,49,52} or react with the allyl radical **10** to form key nucleophilic π -allylcobalt^{II} **12**. Given the experimental results, the combination of the allyl radical **10** and LnCo^{I} **8** represents the major pathway under the current photoredox conditions. Therefore, and based on our previous studies,²³ we tentatively assigned the UV absorption band at 350–460 nm to π -allylcobalt^{II} **12**. It is worth noting that, although the photo-induced homolytic cleavage of the Co–C bond to generate the Co^{II} and C-centered radical species has been well documented previously,⁵³ to the best of our knowledge, the combination of the allyl radical and Co^{I} to produce π -allylcobalt^{II} species under photoredox conditions is unprecedented.³⁰

Based on the above experimental results and previous literature reports, we proposed the catalytic cycle shown in Fig. 3. Initial excitation of 4CzIPN generates the photoexcited $^*4\text{CzIPN}$ species ($E_{1/2} (^*\text{P}/\text{P}^-) = 1.35 \text{ V}$).⁵⁴ In the first SET event, the oxidation of allyl arenes such as **2a** by $^*4\text{CzIPN}$ generates the aryl radical cation **9**, which is then rapidly deprotonated by a base to generate the allyl radical **10**. At the same time, LnCo^{II} **7** is reduced by $4\text{CzIPN}^{\cdot-}$ ($E_{1/2}(\text{P}/\text{P}^-) = -1.21 \text{ V}$) to LnCo^{I} **8**, followed by rapid combination with the allyl radical **10** to produce the key nucleophilic π -allylcobalt^{II} **12** in the SET event. Eventually, the coupling of π -allylcobalt^{II} **12** with the carbonyl group forms a new C–C bond in the alkoxy cobalt product. The protonation of the Co–oxygen bond releases LnCo^{II} **7** and the homoallylic alcohol product to complete the catalytic cycle.

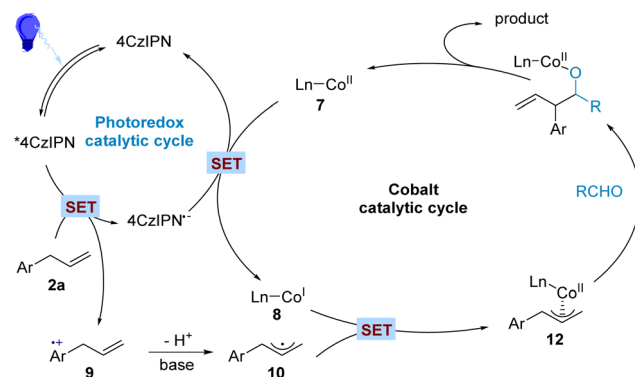


Fig. 3 Proposed catalytic mechanism.

Conclusions

In summary, this study reports a novel photocatalytic redox-neutral synthesis of nucleophilic π -allylcobalt^{II} from easily available unactivated alkenes. This eco-friendly photoredox reaction enables the allylation of various aldehydes, bypassing the use of stoichiometric amounts of reductants such as metals or amines. The success of this reaction depends on the generation of nucleophilic allylcobalt^{II} via the unprecedented combination of allyl radical intermediates and LnCo^{I} complexes under mild photoredox conditions.

Conflicts of interest

There are no conflicts to declare.

Acknowledgements

This project is supported by the National Natural Science Foundation of China (22171036) and the Open Research Fund of School of Chemistry and Chemical Engineering, Henan Normal University (2020YB03).

References

- B. M. Trost, *Science*, 1991, **254**, 1471–1477.
- P. A. Wender and B. L. Miller, *Nature*, 2009, **460**, 197–201.
- G.-L. Li, X.-H. Huo, X.-Y. Jiang and W.-B. Zhang, *Chem. Soc. Rev.*, 2020, **49**, 2060–2118.
- L. Pitzer, J. L. Schwarz and F. Glorius, *Chem. Sci.*, 2019, **10**, 8285–8291.
- P.-S. Wang, M.-L. Shen and L. Gong, *Synthesis*, 2018, **50**, 956–967.
- M. Yus, J. C. González-Gómez and F. Foubelo, *Chem. Rev.*, 2013, **113**, 5595–5698.
- S. E. Denmark and J.-P. Fu, *Chem. Rev.*, 2003, **103**, 2763–2794.

- 8 B. M. Trost and D. L. Van Vranken, *Chem. Rev.*, 1996, **96**, 395–422.
- 9 B. M. Trost and M. L. Crawley, *Chem. Rev.*, 2003, **103**, 2921–2944.
- 10 M. Giedyk, K. Goliszewska and D. Gryko, *Chem. Soc. Rev.*, 2015, **44**, 3391–3404.
- 11 A. Frei, A. P. King, G. J. Lowe, A. K. Cain, F. L. Short, H. Dinh, A. G. Elliott, J. Zuegg, J. J. Wilson and M. A. T. Blaskovich, *Chem. – Eur. J.*, 2021, **27**, 2021–2029.
- 12 J.-F. Han, P. Guo, X.-G. Zhang, J.-B. Liao and K.-Y. Ye, *Org. Biomol. Chem.*, 2020, **18**, 7740–7750.
- 13 M. Kojima and S. Matsunaga, *Trends Chem.*, 2020, **2**, 410–426.
- 14 Z.-J. Wang, Z. Yan, C.-J. Liu and D. W. Goodman, *ChemCatChem*, 2011, **3**, 551–559.
- 15 F. Hebrard and P. Kalck, *Chem. Rev.*, 2009, **109**, 4272–4282.
- 16 T. Sugihara, M. Yamaguchi and M. Nishizawa, *Chemistry*, 2001, **7**, 1589–1595.
- 17 P. J. Chirik, *Acc. Chem. Res.*, 2015, **48**, 1687–1695.
- 18 M. Moselage, J. Li and L. Ackermann, *ACS Catal.*, 2016, **6**, 498–525.
- 19 P. Gomes, C. Gosmini and J. Périchon, *Synthesis*, 2003, 1909–1915.
- 20 K. Michigami, T. Mita and Y. Sato, *J. Am. Chem. Soc.*, 2017, **139**, 6094–6097.
- 21 T. Mita, S. Hanagata, K. Michigami and Y. Sato, *Org. Lett.*, 2017, **19**, 5876–5879.
- 22 A. Gualandi, G. Rodeghiero, R. Perciaccante, T. P. Jansen, C. Moreno-Cabrerizo, C. Foucher, M. Marchini, P. Ceroni and P. G. Cozzi, *Adv. Synth. Catal.*, 2021, **363**, 1105–1111.
- 23 C.-Z. Shi, F.-S. Li, Y.-Q. Chen, S.-J. Lin, E.-J. Hao, Z.-W. Guo, U. T. Wosqa, D.-D. Zhang and L. Shi, *ACS Catal.*, 2021, **11**, 2992–2998.
- 24 À. Cristòfol, B. Limburg and A. W. Kleij, *Angew. Chem., Int. Ed.*, 2021, **60**, 15266–15270.
- 25 S.-J. Xue, À. Cristòfol, B. Limburg, Q. Zeng and A. W. Kleij, *ACS Catal.*, 2022, **12**, 3651–3659.
- 26 B. Limburg, À. Cristòfol and A. W. Kleij, *J. Am. Chem. Soc.*, 2022, **144**, 10912–10920.
- 27 Y.-L. Li, S.-Q. Zhang, J. Chen and J.-B. Xia, *J. Am. Chem. Soc.*, 2021, **143**, 7306–7313.
- 28 X. Jiang, H. Jiang, Q. Yang, Y. Cheng, L.-Q. Lu, J. A. Tunge and W.-J. Xiao, *J. Am. Chem. Soc.*, 2022, **144**, 8347–8354.
- 29 F.-D. Lu, G.-F. He, L.-Q. Lu and W.-J. Xiao, *Green Chem.*, 2021, **23**, 5379–5393.
- 30 L. Wang, L.-F. Wang, M.-X. Li, Q.-L. Chong and F.-K. Meng, *J. Am. Chem. Soc.*, 2021, **143**, 12755–12765.
- 31 H. Xie and B. Breit, *ACS Catal.*, 2022, **12**, 3249–3255.
- 32 Y.-L. Li, W.-D. Li, Z.-Y. Gu, J. Chen and J.-B. Xia, *ACS Catal.*, 2020, **10**, 1528–1534.
- 33 A. Gualandi, G. Rodeghiero, A. Faraone, F. Patuzzo, M. Marchini, F. Calogero, R. Perciaccante, T. P. Jansen, P. Ceroni and P. G. Cozzi, *Chem. Commun.*, 2019, **55**, 6838–6841.
- 34 F.-S. Li, S.-J. Lin, Y.-Q. Chen, C.-Z. Shi, H.-P. Yan, C.-C. Li, C. Wu, L.-Q. Lin, C.-Y. Duan and L. Shi, *Angew. Chem., Int. Ed.*, 2021, **60**, 1561–1566.
- 35 F.-S. Li, Y.-Q. Chen, S.-J. Lin, C.-Z. Shi, X.-Y. Li, Y.-C. Sun, Z.-W. Guo and L. Shi, *Org. Chem. Front.*, 2020, **7**, 3434–3438.
- 36 A. Gualandi, F. Calogero, M. Mazzarini, S. Guazzi, A. Fermi, G. Bergamini and P. G. Cozzi, *ACS Catal.*, 2020, **10**, 3857–3863.
- 37 A. Y. Chan, I. B. Perry, N. B. Bissonnette, B. F. Buksh, G. A. Edwards, L. I. Frye, O. L. Garry, M. N. Lavagnino, B. X. Li, Y.-F. Liang, E. Mao, A. Millet, J. V. Oakley, N. L. Reed, H. A. Sakai, C. P. Seath and D. W. C. MacMillan, *Chem. Rev.*, 2022, **122**, 1485–1542.
- 38 J. Twilton, C. Le, P. Zhang, M. H. Shaw, R. W. Evans and D. W. C. MacMillan, *Nat. Rev. Chem.*, 2017, **1**, 52.
- 39 K. L. Skubi, T. R. Blum and T. P. Yoon, *Chem. Rev.*, 2016, **116**, 10035–10074.
- 40 N. A. Romero and D. A. Nicewicz, *Chem. Rev.*, 2016, **116**, 10075–10166.
- 41 H.-M. Huang, P. Bellotti and F. Glorius, *Chem. Soc. Rev.*, 2020, **49**, 6186–6197.
- 42 J. L. Schwarz, F. Schäfers, A. Tlahuext-Aca, L. Lückemeier and F. Glorius, *J. Am. Chem. Soc.*, 2018, **140**, 12705–12709.
- 43 S. Tanabe, H. Mitsunuma and M. Kanai, *J. Am. Chem. Soc.*, 2020, **142**, 12374–12381.
- 44 H. Mitsunuma, S. Tanabe, H. Fuse, K. Ohkubo and M. Kanai, *Chem. Sci.*, 2019, **10**, 3459–3465.
- 45 H. Cao, Y. Kuang, X.-C. Shi, K. L. Wong, B. B. Tan, J. M. C. Kwan, X.-G. Liu and J. Wu, *Nat. Commun.*, 2020, **11**, 1956.
- 46 Q.-Y. Meng, T. E. Schirmer, K. Katou and B. König, *Angew. Chem., Int. Ed.*, 2019, **58**, 5723–5728.
- 47 X. Hu, G. Zhang, F.-X. Bu and A.-W. Lei, *Angew. Chem., Int. Ed.*, 2018, **57**, 1286–1290.
- 48 J. G. West, D. Huang and E. J. Sorensen, *Nat. Commun.*, 2015, **6**, 10093.
- 49 S. M. Thullen and T. Rovis, *J. Am. Chem. Soc.*, 2017, **139**, 15504–15508.
- 50 T. Lazarides, T. McCormick, P.-W. Du, G.-G. Luo, B. Lindley and R. Eisenberg, *J. Am. Chem. Soc.*, 2009, **131**, 9192–9194.
- 51 P.-W. Du, K. Knowles and R. Eisenberg, *J. Am. Chem. Soc.*, 2008, **130**, 12576–12577.
- 52 H. Cao, H.-M. Jiang, H.-Y. Feng, J. M. C. Kwan, X.-G. Liu and J. Wu, *J. Am. Chem. Soc.*, 2018, **140**, 16360–16367.
- 53 Y. Abderrazak, A. Bhattacharyya and O. Reiser, *Angew. Chem., Int. Ed.*, 2021, **60**, 21100–21115.
- 54 M. A. Bryden and E. Zysman-Colman, *Chem. Soc. Rev.*, 2021, **50**, 7587–7680.